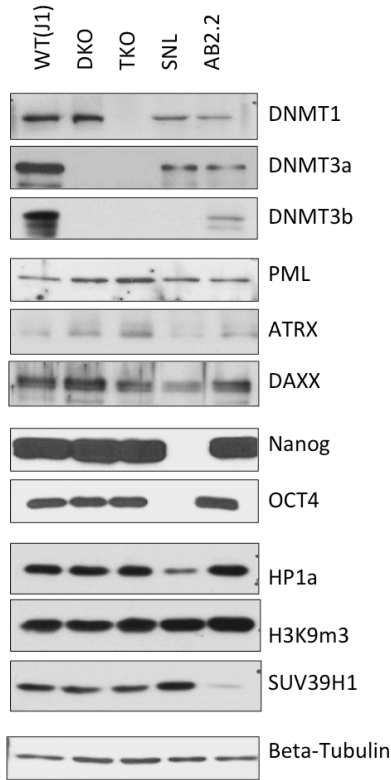
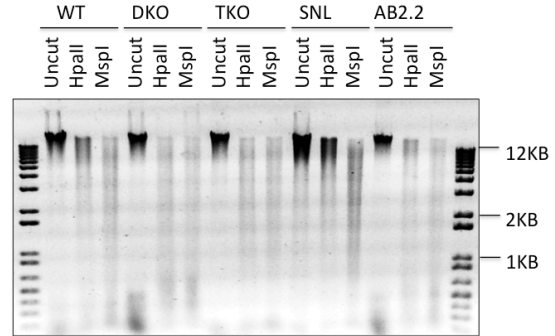


Figure S1

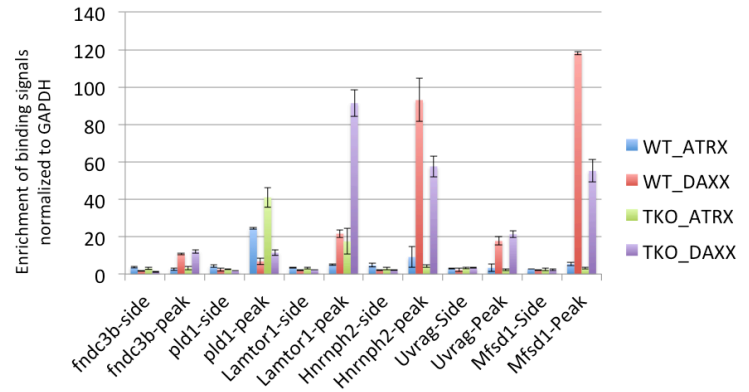
A



B



C



D

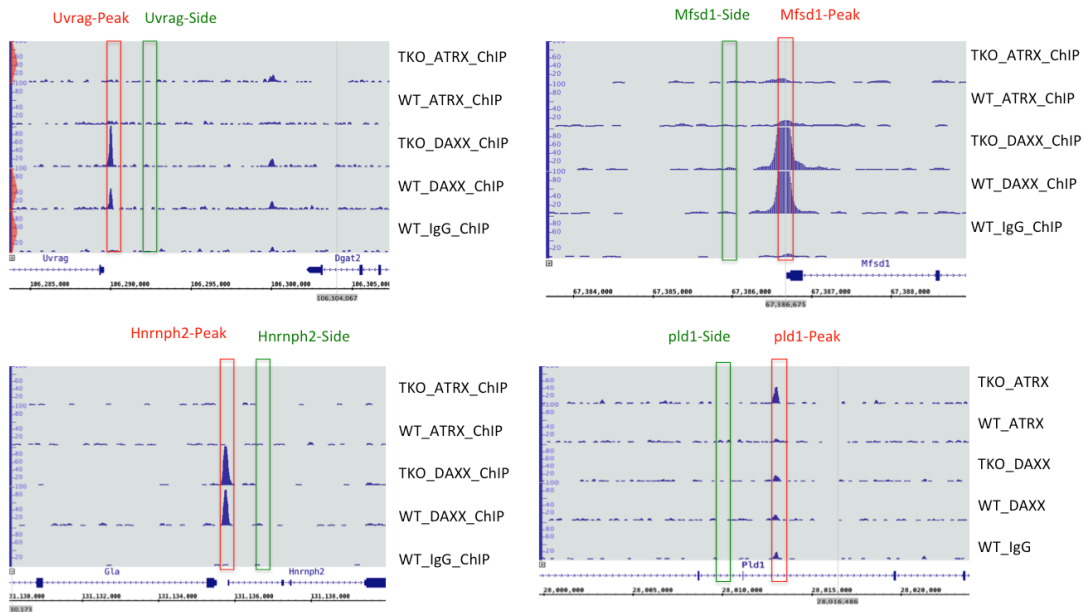
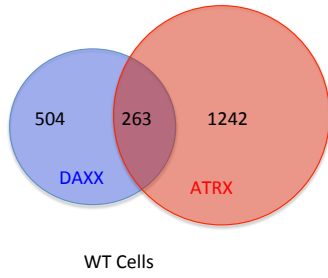


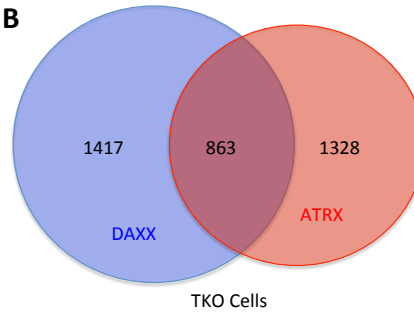
Figure S1. Related to Figure 1. **(A)** Wildtype (WT) J1 mES cells, J1 cells double knocked out for DNMT3a/DNMT3b (DKO), and J1 cells triple knocked out for DNMT1/3a/3b (TKO) were used in this study. The cells were western blotted with the indicated antibodies. Another mES cell line AB2.2 and the immortalized mouse fibroblast cell line SNL served as controls. **(B)** Cells from (A) were subjected to restriction digestion (HpaII vs. MspI) for DNA methylation status analysis. **(C)** ChIP-Seq results from wildtype J1 and TKO cells were validated by ChIP-qPCR experiments using the indicated primers for 6 peaks and 6 side regions. **(D)** Snapshots showing four of the six regions from (C) with peaks for DAXX/ATRX and primer targeting regions.

Figure S2

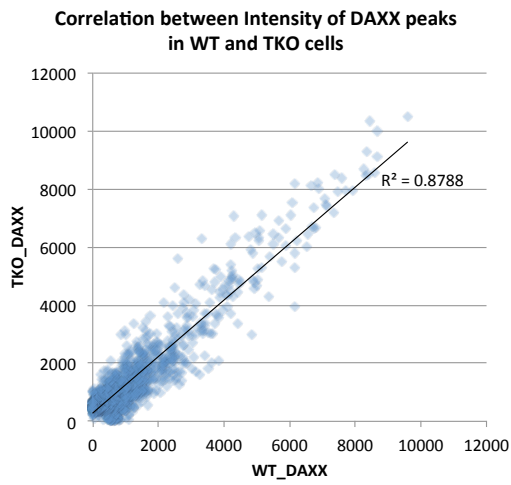
A



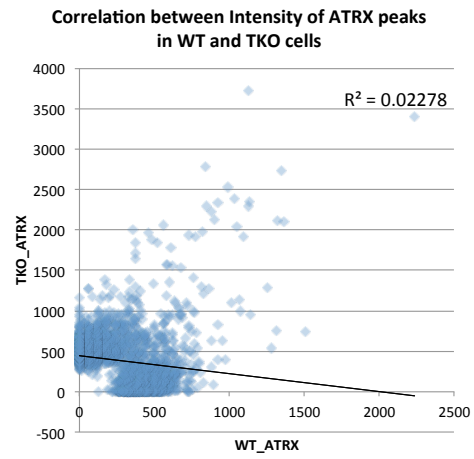
B



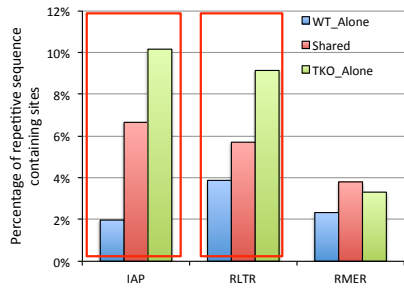
C



D



E



F

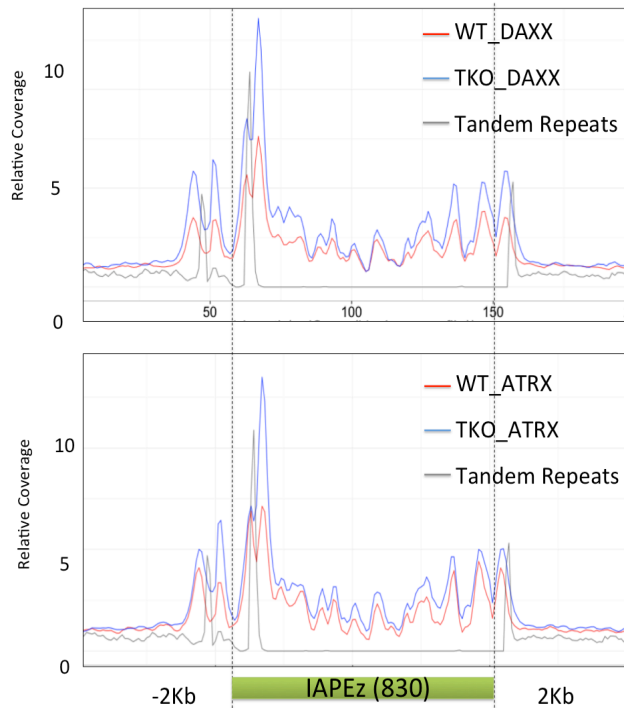


Figure S2. Related to Figure 2. **(A-B)** Analysis of DAXX and ATRX binding sites identified from genome-wide ChIP-seq experiments. The DAXX and ATRX binding sites identified in wildtype J1 (A) and TKO cells (B) show some degree of overlap. **(C-D)** Scatter plots of binding intensity (normalized reads coverage) of DAXX (C) and ATRX (D) on their binding regions in WT and TKO cell lines. Trendlines were calculated by linear regression to examine the correlation of binding profiles. R^2 indicates the degree of correlation in coverage depth (intensity) of the examined binding sites between wildtype J1 (WT) and TKO cells for DAXX and ATRX. **(E)** The percentages of ERVK family repeats found in DAXX-binding sites shared between wildtype J1 (WT) and TKO cells (Shared) or unique for each cell type (WT_Alone or TKO_Alone) were plotted. **(F)** The ATRX and DAXX binding profiles across the 830 IAPEz and 640 MERVL elements (within +/- 2kb regions) in J1 and TKO cells are plotted here. The grey line indicates the accumulated distribution of tandem repeats.

Figure S3

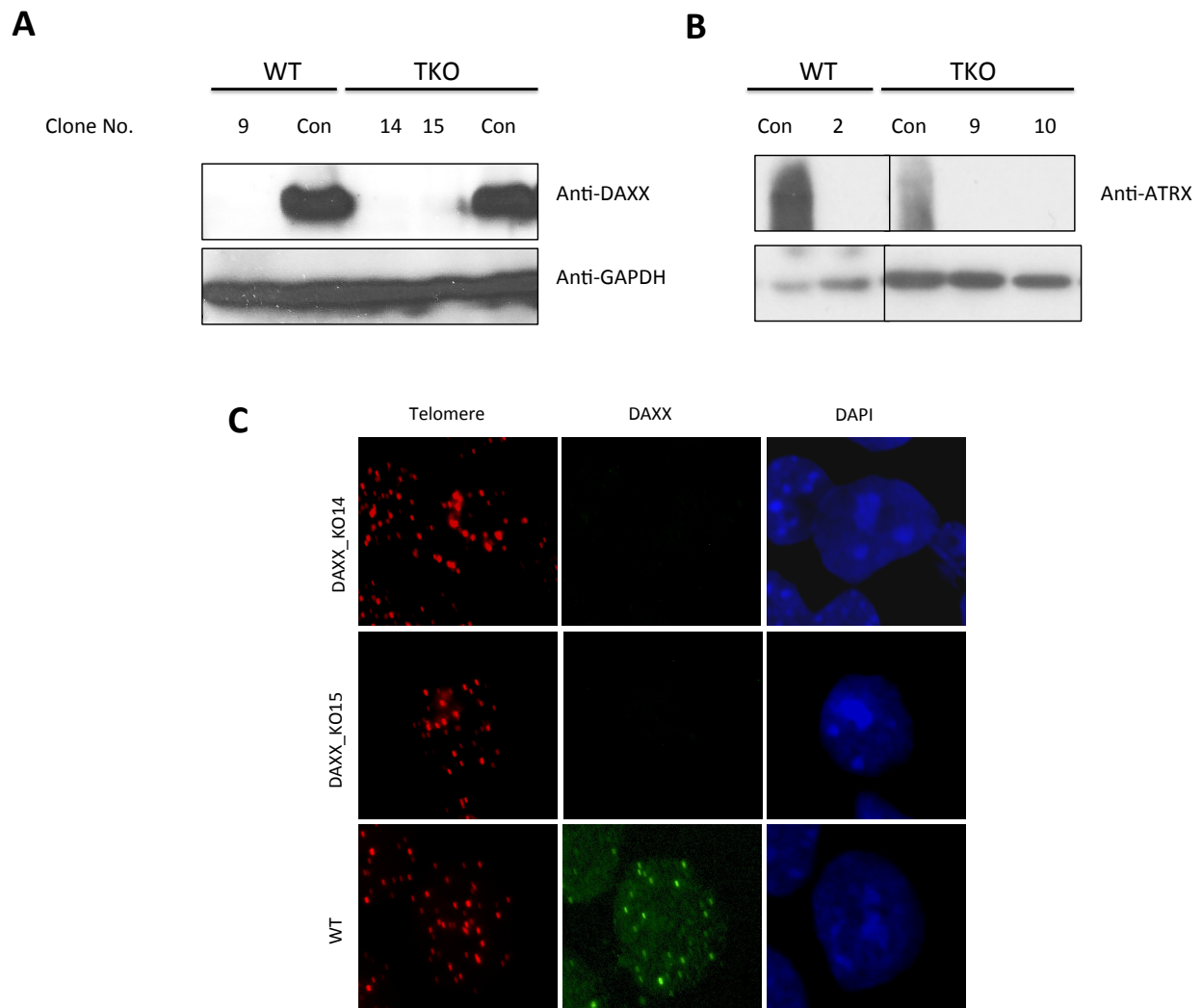
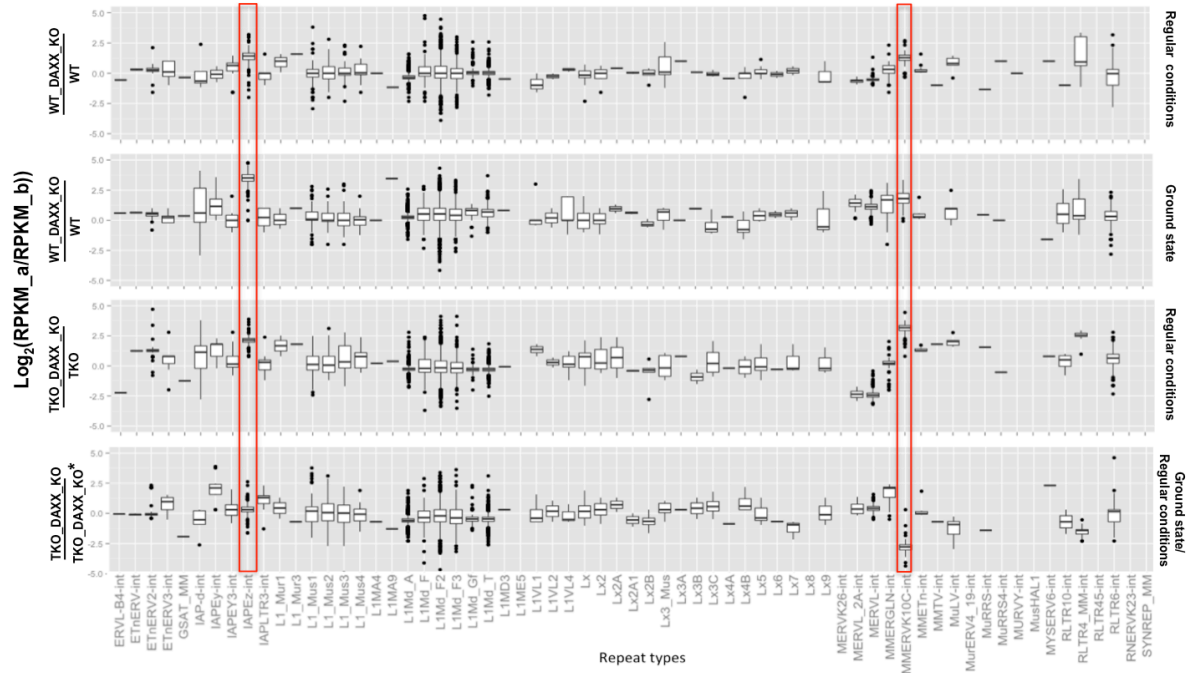


Figure S3. Related to Figure 2. **(A-B)** Analysis of wild type J1 cells (WT) and TKO cells knocked out for DAXX or ATRX. Expression of DAXX (A) and ATRX (B) in the knockout clones was examined by western blotting with the indicated antibodies. **(C)** DAXX knockout clones #14 and #15 were immunostained with antibodies against endogenous DAXX (green) and a telomere PNA probe (red). DAPI was used to stain the nuclei.

Figure S4

A



B

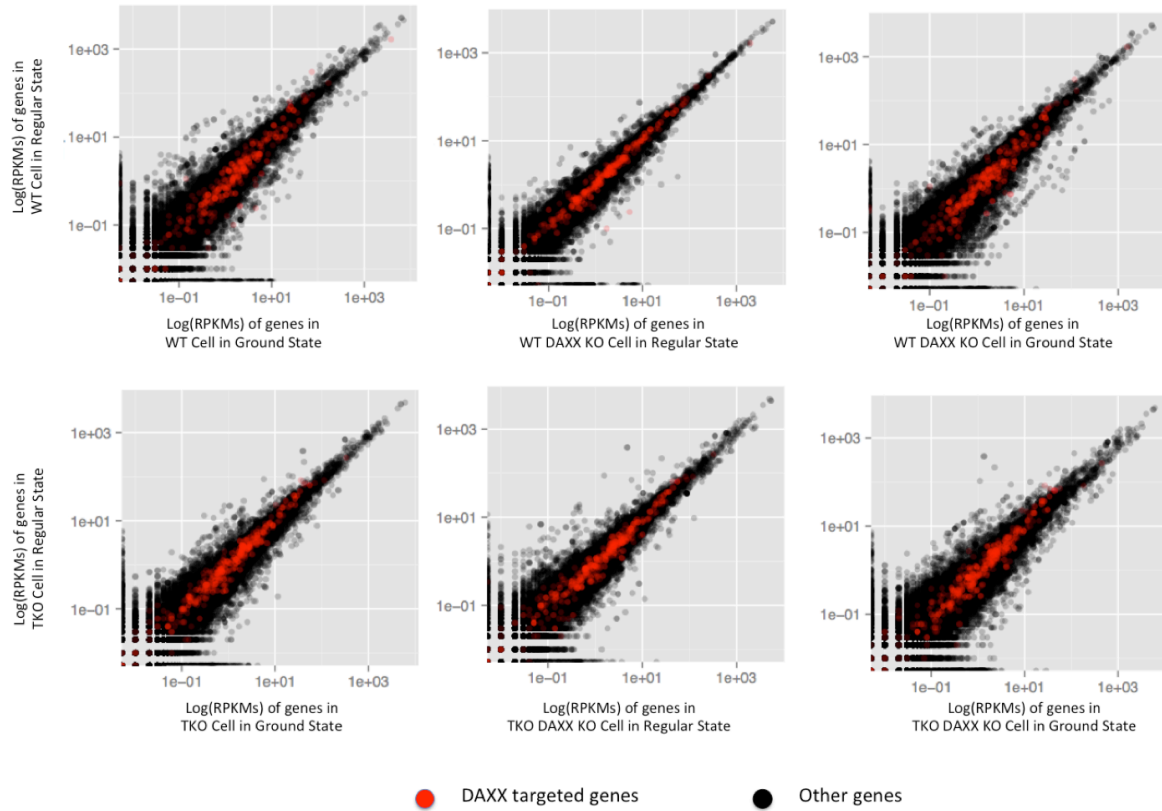


Figure S4. Related to Figure 3. Comparison of expression levels of DAXX targeting repetitive elements and genes across different cell lines. RNA-seq experiments were carried out using wildtype J1, wildtype DAXX KO, TKO, and TKO DAXX KO cells grown under regular vs. ground-state (2i+vitamin C (VC)) conditions. **(A)** The transcriptional levels of repetitive elements were compared and plotted as shown. Various repeat types were plotted on the x-axis, and the ratios of RPKMs (Reads Per Kilobase of transcript per Million mapped reads) of the two samples plotted on the y-axis (log₂ scale). Red boxes indicate specific IAP and LTR families that we found to be targeted by DAXX. The classification and names of repetitive element classes follows Repbase (Jurka et al., 2005). **(B)** Pairwise comparisons of the RPKMs (Reads Per Kilobase of transcript per Million mapped reads) of various samples plotted on the log₁₀ scale in scatter plots. Wildtype J1 (WT) and TKO cells as well as J1 and TKO cells knocked out for DAXX were grown in regular or ground-state media and examined for the transcriptional levels of DAXX target vs. non-target genes. The red dots represent DAXX target genes (DAXX binding to their promoter regions) and the black dots represent non-target genes. No significant differences were observed for DAXX target genes in these comparisons.

Figure S5

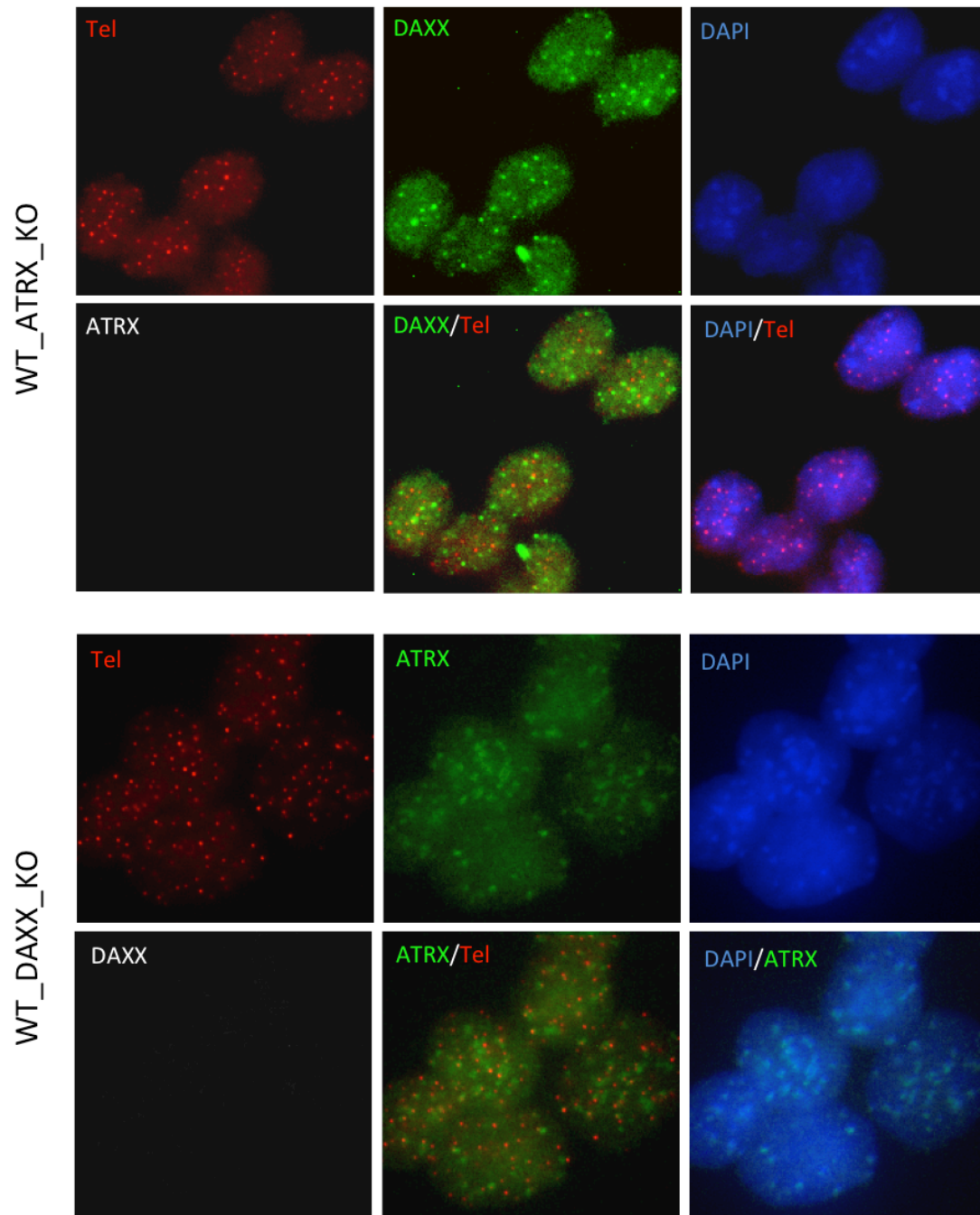


Figure S5. Related Figure 4. Immunostaining analysis of DAXX and ATRX in wildtype J1 cells knocked out (KO) for DAXX or ATRX. Cells were co-stained with anti-DAXX and anti-ATRAX antibodies together with a telomere probe (Tel). DAPI was used to stain the nuclei. Images in the bottom panels of each cell line highlight the success of individual gene KO as well as its effect on the telomere localization of the other protein.

Figure S6

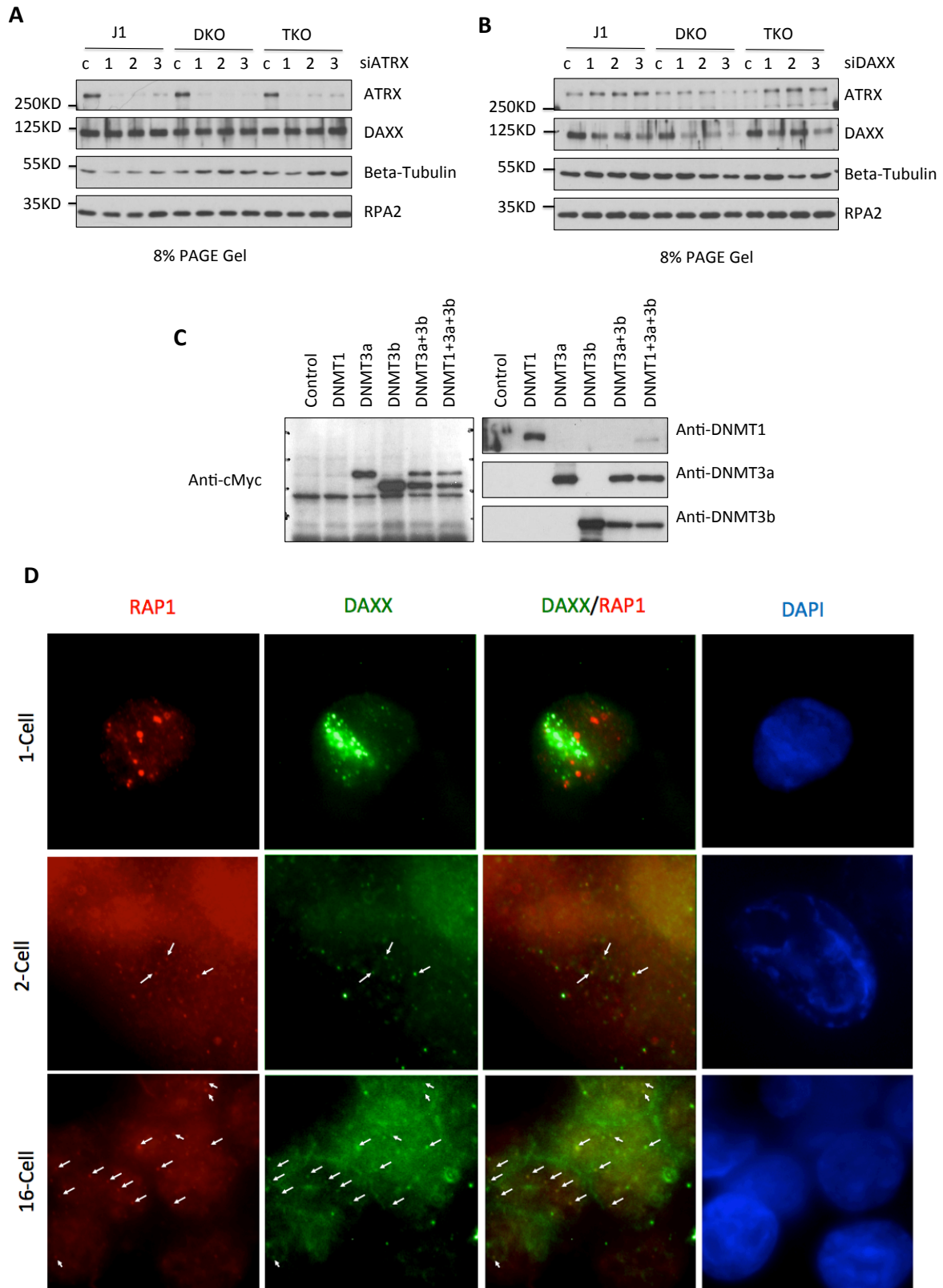


Figure S6 Related Figure 4. **(A-B)** Knockdown efficiency of the ATRX and DAXX siRNAs in wildtype J1 (WT) and TKO cells was determined by western blotting. **(C)** Expression of cMyc-tagged DNMT proteins in TKO cells in the rescue experiments was determined by western blotting. *, non-relevant sample. **(D)** Immunostaining analysis of pre-implantation embryos with antibodies against DAXX and RAP1. The telomere-binding protein RAP1 served as a marker for telomeres. White arrows indicate co-localized foci.

Figure S7

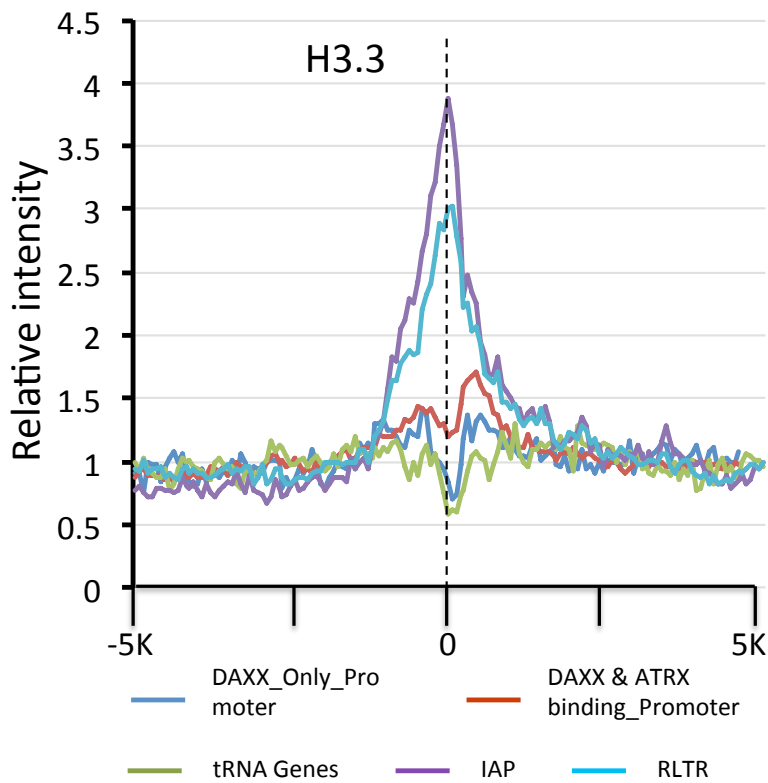


Figure S7. Related to Figure 7. The binding profiles of H3.3 on distinct DAXX and ATRX binding sites (colored as shown, ± 5 kb from the binding peaks) in WT mES cells. The classification of binding sites was based on our DAXX and ATRX ChIP-seq data. H3.3 ChIP-seq data were adapted from published data (supplemental Table S3). The center vertical dotted line indicates the summit of binding peaks.

Supplemental Tables

Supplementary Table S1. Related to Figure 4. List of siRNAs

Name	Sequence (5'-3')
siDAXX_1	GUAACUCCGGUAGUAGGAA[dT][dT] UUCCUACUACCGGAGUUAC[dT][dT]
siDAXX_2	CUUAGCUCCUGCAGCCUCA[dT][dT] UGAGGCUGCAGGAGCUAAG[dT][dT]
siDAXX_3	GCUAAGAUCUAUGUGUACA[dT][dT] UGUACACAUAGAUCUAGC[dT][dT]
siATRX_1	GAUGCUAGAUCAUCAGUAA[dT][dT] UUACUGAUGAUCUAGCAUC[dT][dT]
siATRX_2	CUCUAAGAGUUUAAGCUCA[dT][dT] UGAGCUUAAACUCUAGAG[dT][dT]
siATRX_3	CCAAAGAAGAGUAGUUCUA[dT][dT] UAGAACUACUCUUCUUUGG[dT][dT]
siNeg	siRNA Universal negative control (Sigma)

Supplementary Table S2. Related to Figure 2. Primer sets for CRISPR plasmid construction

Name	Gene	Exon/Strand	Sequence (5'-3')
mATRX_Cri_330_2_F	Mouse ATRX	Exon1/+	CACCG AAAAGCAAATCAGAAACGCG
mATRX_Cri_330_2_R	Mouse ATRX	Exon1/+	AAAC CGCGTTTCTGATTTGCTTTT C
mDAXX_Cri_330_1_F	Mouse DAXX	Exon1/+	CACCG GGCCACACAGTGCGACCCGG
mDAXX_Cri_330_1_R	Mouse DAXX	Exon1/+	AAAC CCGGGTTCGCACTGTGTGGCCC
mDAXX_Cri_330_2_F	Mouse DAXX	Exon1/+	CACCG CTCTCCGGGTTCGCACTGTG
mDAXX_Cri_330_2_R	Mouse DAXX	Exon1/+	AAAC CACAGTGCGACCCGGAGGAG C

Supplementary Table S3. Related to Figure 1-3. List of all GEO datasets used in the study.

SRA Run ID	Description	Ref.
SRR006831	H3K4me3 ChIP in WT mES cell	(Mikkelsen et al., 2007)
SRR007435	H3K9me3 ChIP in WT mES cell	(Mikkelsen et al., 2007)
SRR036749 (GSM515676)	Pol 2 ChIP in WT mES cell	(Mikkelsen et al., 2007)
SRR057606 (GSM555160)	TBP ChIP in WT mES cell	
SRR036139 SRR036140 SRR036141	H3.3 (HA) ChIP in WT mES cell	(Goldberg et al., 2010)

SRR070936 (GSM611203)	DNA methylation bisulfide sequencing in WT mES cell	(Williams et al., 2011)
SRR070941 (GSM611208)	DNA methylation bisulfide sequencing in TKO mES cell	(Williams et al., 2011)
SRR599648 (GSM727427)	J1_WT_mRNA-Seq	(Karimi et al., 2011)
GSM727427 (GSM727428)	J1_DNMT_TKO_mRNA-Seq	(Karimi et al., 2011)

Supplementary Table S4. Related to Experimental Procedures. List of antibodies used in the study.

Antigen	Cat. #	Source	Assay	Source
H3.3 (phosphor S31)	ab62207	Abcam	WB, ChIP	Rb
ATRX	SC-15408	Santa Cruz	ChIP, IF, WB	Rb
ATRX	SC-55584	Santa Cruz	IF	Ms
DAXX	SC-7152	Santa Cruz	ChIP, IF, WB	Rb
DAXX	SC-7000	Santa Cruz	IF	Ms
DNMT1	SC-20701	Santa Cruz	WB	Rb
DNMT3a (H-295)	SC-20703	Santa Cruz	WB	Rb
DNMT3b	SC-52922	Santa Cruz	WB	Ms
PML(N-19)	SC-9862	Santa Cruz	WB	Gt
RAP1	A300-306A	Bethyl Laboratories	ChIP, IF	Rb
H3K9me3	Ab8898	Abcam	ChIP,	Rb
H3K9me3	07-442	Upstate	ChIP, IF	Rb
HP1a	2616	Cell Signaling	ChIP, IF	Rb
HP1a	39978	Active Motif	WB, IF	Ms
FLAG	F7425	Sigma-Aldrich	WB, IP, IF	Rb
GST	95038-580	VWR	WB	Ms
RPA2	A300-245A	Bethyl Laboratories	WB	Rb
Beta-tubulin	EP1331Y	EPITOMICS	WB	Rb
Nanog	Ab21624	Abcam	WB	Rb
Oct4	Ab19857	Abcam	WB	Rb
GAPDH	2251-1	EPITOMICS	WB	Rb
SUV39H1	8729s	Cell Signaling	WB	Rb

Supplementary Table 5. Related to Experimental Procedures. Primer sets for ChIP-PCR

Name	Sequence (5'-3')
Uvrag-Peak-F	TCCCTATTGAGGGGTGTGGT
Uvrag-Peak-R	ACGTGACACGACATACCAGG
Uvrag-Side-F	GCCTTTACCACAGACCTGCT
Uvrag-Side-R	CGGATCCAGGGACGAATCAG
Mfsd1-Peak-F	CCCCATCGGCAGAACAGAAA

Mfsd1-Peak-R	CGTGTGTTACGTGACTTGC
Mfsd1-Side-F	GGCGCTGTGTTGTTCTTGT
Mfsd1-Side-R	TACAGGTGCACGTTAGCTGG
Hnrnp2-Peak-F	TGGCGCTCTCTTACCTGG
Hnrnp2-Peak-R	AACGAGACCGGGGATTTTC
Hnrnp2-Side-F	GCATTCATCCCTTGGGCTC
Hnrnp2-Side-R	ACTGACTAAGCAATCTGCCCC
Lamtor1-Peak-F	AGTACGCTACTCGCCACTTG
Lamtor1-Peak-R	CAGCCAAATCTTGCCTTCCG
Lamtor1-Side-F	GTAAGTGGGAAGCTGGTGGG
Lamtor1-Side-R	TCCTTGCTCTGGTTCAGACC
Pld1-Peak-F	AGCATTGAGAGAGGGAGAGGA
Pld1-Peak-R	AGTTGTCCTTGCACACGCTG
Pld1-Side-F	GCATTCATCCCTTGGGCTC
Pld1-Side-R	ACTGACTAAGCAATCTGCCCC
Fndc3b-Peak-F	CCTAGCACAGCATGGGAGTT
Fndc3b-Peak-R	TGGAGTACCTGTGGCCTACT
Fndc3b-Side-F	TTAGATGCTACCAGCCCCA
Fndc3b-Side-R	GCTTACCGAGACGCGAGATA
Capn2-Peak-F	TGCCATAGCTCTGTCTCACG
Capn2-Peak-R	TCCGGTCCCTTGTGGTGGAC
Capn2-Side-F	AAGCCTGGTACTCCTCTCCC
Capn2-Side-R	GCAAAGGGGTGGATAAGGGT
tRNA-TTG-Peak-F	ACAGGAACTTTTGTGACGCT
tRNA-TTG-Peak-R	ATAGAGATTGCCCCAGCACC
tRNA-TTG-Side-F	ATGACCAAGAGGAAGCAGCC
tRNA-TTG-Side-R	TCAGATGCCCTCAGACTGGA

Supplementary Table 6. Related to Experimental Procedures. Primer sets for qRT-PCR

Name	Sequence (5'-3')	Targets
IAP-1-qRT-PCR-F	GCACCCTCAAAGCCTATCTTA	IAP transcription
IAP-1-qRT-PCR-R	TCCCTTGGTCAGTCTGGATTT	IAP transcription
tRNA998_qRT-PCR_F	GCGttGGtGGtAtAGtGG	tRNA transcription
tRNA998_qRT-PCR_R	TTGGCCGGGaaTCGaaCC	tRNA transcription
tRNA398_qRT-PCR_F	CTCGTGGCGCAACGGTAGC	tRNA transcription
tRNA398_qRT-PCR_R	CGACGTGATTTGAACACGCA	tRNA transcription
tRNA401_qRT-PCR_F	GTAGCGTGGCCGAGCGGTct	tRNA transcription
tRNA401_qRT-PCR_R	CAGCGGTGGGATTCGAACCC	tRNA transcription

tRNA626_qRTPCR_F	TCCCTGGTAGTCTAGTGG	tRNA transcription
tRNA626_qRTPCR_R	CTGACTAGGATTCAAACCT	tRNA transcription
tRNA371_qRTPCR_F	GGGGATGTAGCTCAGTGG	tRNA transcription
tRNA371_qRTPCR_R	AGATGCCGGGAATCGAACC	tRNA transcription
m11q-TERRA-Genome-F	CTGCTGAGGTCCACAGATCC	Measure TERRA transcription
m11q-TERRA-Genome-R	TCATGAGTGTGGTTCTCGCC	Measure TERRA transcription
m18q-TERRA-Genome-F	AGTTCATGGTGACAAGCTGC	Measure TERRA transcription
m18q-TERRA-Genome-R	GAAGGGACAGACTGACACTGG	Measure TERRA transcription
m5q-TERRA_Genome_F	GGAAGCCAGGGCATAATGGA	Measure TERRA transcription
m5q-TERRA_Genome_R	GGTGCCCTCACAACCTCATCA	Measure TERRA transcription
RTPCR_mATRX	CAAAATGGCGTCGGCATAGG	ATRX
RTPCR_mATRX	GAAGTCCATCTTCTCCGCGT	ATRX
RTPCR_mDAXX	ACCGTTTCTGAGGGGAATTTGA	DAXX
RTPCR_mDAXX	GGTCAACGCCTGGCCTAT	DAXX
mUvrq-RTPCR-1-F	CATCGCTGCTCGGAACATTG	Uvrq
mUvrq-RTPCR-1-R	TGCGTTTGGATGACCCTTGT	Uvrq
mMfsd1-qRTPCR-1-F	GAGGTCCTCAACCGCTCAA	Mfsd1
mMfsd1-qRTPCR-1-R	TGTCTTGGCGTTTGGCTAGA	Mfsd1
mHnrnp2-qRTPCR-1-F	GTTGGAGTCCTGCAGCAAACA	Hnrnp2
mHnrnp2-qRTPCR-1-R	ATGCTTCACCACTCGGTCTG	Hnrnp2
mGla-qRTPCR-1-F	CATGTGCAACCTTGACTGCC	Gla
mGla-qRTPCR-1-R	TGTGGACGTAATTTGCGAGGT	Gla
mLamtor1-qRTPCR-1-F	TTAGGACAGGCTAGGCGAGG	Lamtor1
mLamtor1-qRTPCR-1-R	GCGGGTACTGTACTGCCTTG	Lamtor1
mFndc3b-qRTPCR-1-F	GCCTACAGTGGATCGGCTAC	Fndc3b
mFndc3b-qRTPCR-1-R	GACCGTACCCTCCGTCATTC	Fndc3b
mCapn2-qRTPCR-1-F	GGCCCTACTCCAGCAAACCT	Capn2
mCapn2-qRTPCR-1-R	AGCACCCATTGATCTTGGCA	Capn2
mNanog-qRTPCR-F	cagtctggacactggctgaa	Nanog
mNanog-qRTPCR-R	ctcgctgattaggctccaac	Nanog

Supplementary Table S7. Related to Figure 3. Primer/Oligo sets for KD and qRT-PCR in embryos

siATRX_1	GAUGCUAGAUAUCAGUAA[dT][dT]
	UUACUGAUGAUCUAGCAUC[dT][dT]
mGapdh 5' primer	CCATCAACGACCCCTTCATTGACC
mGapdh 3' primer	TGGTTCACACCCATCACAAACATG
IAP-F	AAGCCCTTTTGTTCCTTTTCA
IAP-R	ACCCTTGGAAGGCCTGTAT

Supplemental Experimental Procedures

ChIP-seq and data analysis

The quantity and size distribution of the libraries were determined using the PicoGreen fluorescence assay and the Agilent 2100 Bioanalyzer, respectively. The quality of the library was assessed by determining the enrichment of known target regions with real-time PCR. Sequencing of the library was carried out on the Illumina Genome Analyzer system.

Low quality reads were filtered and adaptor sequences were trimmed using our in-house perl script. Alignment of short reads (100bp) to the mouse genome (mm9 release, UCSC) was done using Bowtie 2 (Langmead and Salzberg, 2012; Langmead et al., 2009), with a sensitive-local, paired-end model. All PCR duplicates were removed using Picard. The MACS software (Zhang et al., 2008) was used to recognize peaks (with $e=1e-6$ and fold-enrichment of >2 as cutoff). The UCSC genome database was used to annotate the identified peaks for genomic features. Promoters were defined as ± 0.5 kb relative to the start of UCSC gene transcription start sites. The definition of mouse ancestral simple repeat sequences was downloaded from Repbase (Jurka et al., 2005). Two peaks with a distance of <50 bp are considered overlapping. Gene classification and functional analyses were done by R using Bioconductor packages including ChIPpeakAnno and BSgenome.Mmusculus.UCSC.mm9. Motif search for binding sites was done by the MEME-ChIP server (<http://meme.nbcr.net/meme/cgi-bin/meme-chip.cgi>). Average binding profiles were calculated by summing the coverage depth of all targeted regions based on the wig files from MACS, which were normalized by dividing with the median value of non-binding regions. Heat maps were drawn using a R script developed in-house based on these normalized binding profiles.

RNA-seq and data analysis

The mouse reference genome, transcriptome, and annotation data were downloaded from Illumina iGenomes (version: UCSC mm9, download time: 2015/3/10). Repetitive element definition and location were downloaded from UCSC genome tab browser (RepeatMasker). Paired-end RNA-seq reads were aligned to the genome (mm19) using Tophat with default parameters (Bowtie2 (version 2.2.4) for alignment). Transcript assembly was done by Cufflinks and then all the assembly files from each sample were merged to a reference annotation-based transcript assembly for use in downstream differential analysis. Differential analysis was done by Cuffdiff, which calculates expression in two or more samples and tests the statistical significance of each transcript. To compare the expression level of transcripts across samples, we used RPKM (Reads Per Kilobase per Million mapped reads) to represent expression levels with the formula $RPKM = (10^9 * C)/(N * L)$, where C is the number of reads mapped to a gene, N is the total number of reads mapped to all exons in the genome, and L is exon length in base-pairs for a gene. For expression analysis of repetitive elements, all elements <5Kbps in length were removed. The RPKMs for each repetitive element and the DAXX/ATRX binding profiles on these regions were calculated by a homemade R script. Only unique/best-matched reads were used to calculate RPKMs for repetitive elements to avoid multiple alignments. The plots of RPKMs were drawn using the ggplot package in R.

Chromatin Immunoprecipitation (ChIP), telomere ChIP, ChIP-qPCR, and RT-qPCR

ChIP assays were performed essentially as previously described (Nelson et al., 2006). Briefly, $\sim 1 \times 10^7$ mES cells were fixed and permeabilized with 4% paraformaldehyde for 10 min at 4°C before lysis and sonication. Sonicated and pre-cleared lysates were incubated with

appropriate antibodies before the addition of Protein A agarose beads. The efficiency and specificity of the antibodies were confirmed by western blotting. A list of the antibodies used in this study can be found in supplementary Table S1. The precipitated DNA was then eluted and analyzed by deep-sequencing, dot-blotting, qPCR, or telomere-ChIP as described previously (Ma, 2011). A radiolabeled oligonucleotide probe (TTAGGG)₃ was used to detect telomeric DNA by southern blotting. The primers used in ChIP-PCR are listed in supplementary Table S2.

For RT-qPCR, total RNA was isolated (RNeasy Mini Kit, Qiagen) and reverse transcribed using the iScript cDNA Synthesis Kit (Bio-Rad). Real-time qPCR was carried out using an ABI StepOnePlus real-time PCR system and the SYBR green master mix (Applied Biosystems). The qRT-PCR primers used in this study are listed in supplementary Table S3. Three independent biological repeats were obtained for each sample to arrive at statistical means and standard deviation. We used a moderated *t*-test to calculate *p*-values. A *p*-value of <0.05 is considered significant.

Immunofluorescence *in situ* hybridization (Immuno-FISH), quantitative FISH (Q-FISH), and Chromosome Orientation FISH (CO-FISH) assays

For telomere FISH, cells were doubly fixed and permeabilized with 4% paraformaldehyde and 5% Triton X-100 before incubation with antibodies and the telomere PNA probe (Bio-PNA), and visualized on a Nikon PCM 2000 confocal microscope. FISH hybridization of metaphase spreads (≥ 30 metaphases per sample) were performed as previously described, which were visualized on a Nikon TE200 fluorescence microscope and analyzed with TFL-TELO (Leica Imaging Systems). For chromosomal aberrations and karyotyping, ≥ 50 metaphases per sample were analyzed (Rebuzzini et al., 2008).

Co-FISH assays were performed as described previously (Bailey et al., 2010) with minor modifications. Cells were first labeled with 5'-BrdU and 5'-BrdC (3:1) for 16-20 hours before addition of nocodazole (0.5µg/ml) for 1.5~3h, resuspended in hypotonic solution (0.075M KCL) for 25min at 25°C, and then fixed with methanol and glacial acetic acid (3:1) for 3-5 mins before being spread onto glass slides and dried overnight. The slides were then rehydrated in 1xPBS for 4 min at 25°C, treated with RNase (54ng/µl) for 10 min at 37°C and then pepsin solution (10mM HCl and 125µl of 1% pepsin in 50mls) for 1-2 mins. The slides were further fixed and stained with Hoechst 33258 (Sigma) for 15mins at 25°C before being exposed to 365 nm UV for 35min at 50°C. After ExoIII treatment, the slides were placed at 85°C for 3mins before incubation with telomere PNA probes (TelC(CCCTAA)₃-FAM and TelG(TTAGGG)₃-Cy3)(PNA Bio) at 25°C for 2hrs. At least 50 metaphase spreads were captured for each sample by a Nikon TE200 fluorescence microscope.

Immunostaining using whole embryo mount

Early zygotes and pre-implantation stage embryos were obtained following *in vitro* fertilization, and *in vivo* derived eggs were cultured in KSOM medium as described previously (Garrick et al., 2006). C57/B6 female mice superovulated with 5 IU PMSG and 5 IU hCG 46 hours were used for breeding. Collected zygotes were fixed in 4% paraformaldehyde (PFA) for 30 min, washed with 1xPBS containing 10 mg/mL BSA, and permeabilized with 1% Triton X-100 for 20 min before incubation with primary and secondary antibodies. After washing three times, embryos were fixed with 4% paraformaldehyde for 5 mins, washed three times 0.1% BSA/PBS and then denatured at 85°C for 4 min and hybridized to (TTAGGG)₃ probes labeled with Cy3 for 2 hours at room temperature. The cells were washed and mounted onto glass slides

in Vectashield anti-bleaching DAPI mounting solution (Vector Laboratories, Burlingame, CA). For knockdown experiments, siRNA oligos (20 μ M) (supplemental Table S7) were injected into the cytoplasm of zygotes using the Femojet microinjection system (Eppendorf). The zygotes were then cultured in KSOM medium for 48 hours before analysis.

Whole transcriptome amplification using morula-stage embryos

Whole transcriptome amplification of embryos was performed using the PEPLI-g WTA Single Cell Kit (Qiagen,150063). Briefly, ~20 morula-stage embryos were transferred into PCR tubes containing 1xPBS (7 μ L), followed by the addition of 4 μ L lysis buffer. The reaction mixtures were incubated at 95 $^{\circ}$ C and treated with genomic DNA wipeout buffer to remove genomic DNA. Following cDNA synthesis and amplification, the product was diluted 100 fold, of which 2-3 μ L of the diluted product was used for real-time qPCR. The primers and oligo sequences can be found in supplemental Table S7.

References

- Bailey, S.M., Williams, E.S., Cornforth, M.N., and Goodwin, E.H. (2010). Chromosome Orientation fluorescence in situ hybridization or strand-specific FISH. *Methods Mol Biol* 659, 173-183.
- Garrick, D., Sharpe, J.A., Arkell, R., Dobbie, L., Smith, A.J., Wood, W.G., Higgs, D.R., and Gibbons, R.J. (2006). Loss of Atrx affects trophoblast development and the pattern of X-inactivation in extraembryonic tissues. *PLoS Genet* 2, e58.
- Goldberg, A.D., Banaszynski, L.A., Noh, K.M., Lewis, P.W., Elsaesser, S.J., Stadler, S., Dewell, S., Law, M., Guo, X., Li, X., *et al.* (2010). Distinct factors control histone variant H3.3 localization at specific genomic regions. *Cell* 140, 678-691.
- Jurka, J., Kapitonov, V.V., Pavlicek, A., Klonowski, P., Kohany, O., and Walichiewicz, J. (2005). Repbase Update, a database of eukaryotic repetitive elements. *Cytogenetic and genome research* 110, 462-467.
- Karimi, M.M., Goyal, P., Maksakova, I.A., Bilenky, M., Leung, D., Tang, J.X., Shinkai, Y., Mager, D.L., Jones, S., Hirst, M., *et al.* (2011). DNA methylation and SETDB1/H3K9me3 regulate predominantly distinct sets of genes, retroelements, and chimeric transcripts in mESCs. *Cell stem cell* 8, 676-687.
- Langmead, B., and Salzberg, S.L. (2012). Fast gapped-read alignment with Bowtie 2. *Nature methods* 9, 357-359.
- Langmead, B., Trapnell, C., Pop, M., and Salzberg, S.L. (2009). Ultrafast and memory-efficient alignment of short DNA sequences to the human genome. *Genome biology* 10, R25.
- Ma, W. (2011). Analysis of telomere proteins by Chromatin Immunoprecipitation (ChIP). *Methods Mol Biol* 735, 151-159.
- Mikkelsen, T.S., Ku, M., Jaffe, D.B., Issac, B., Lieberman, E., Giannoukos, G., Alvarez, P., Brockman, W., Kim, T.K., Koche, R.P., *et al.* (2007). Genome-wide maps of chromatin state in pluripotent and lineage-committed cells. *Nature* 448, 553-560.
- Nelson, J.D., Denisenko, O., and Bomsztyk, K. (2006). Protocol for the fast chromatin immunoprecipitation (ChIP) method. *Nature protocols* 1, 179-185.
- Rebuzzini, P., Neri, T., Zuccotti, M., Redi, C.A., and Garagna, S. (2008). Chromosome number variation in three mouse embryonic stem cell lines during culture. *Cytotechnology* 58, 17-23.
- Williams, K., Christensen, J., Pedersen, M.T., Johansen, J.V., Cloos, P.A., Rappsilber, J., and Helin, K. (2011). TET1 and hydroxymethylcytosine in transcription and DNA methylation fidelity. *Nature* 473, 343-348.
- Zhang, Y., Liu, T., Meyer, C.A., Eeckhoutte, J., Johnson, D.S., Bernstein, B.E., Nusbaum, C., Myers, R.M., Brown, M., Li, W., *et al.* (2008). Model-based analysis of ChIP-Seq (MACS). *Genome biology* 9, R137.